Zheng et al., http://www.jcb.org/cgi/content/full/jcb.201001148/DC1

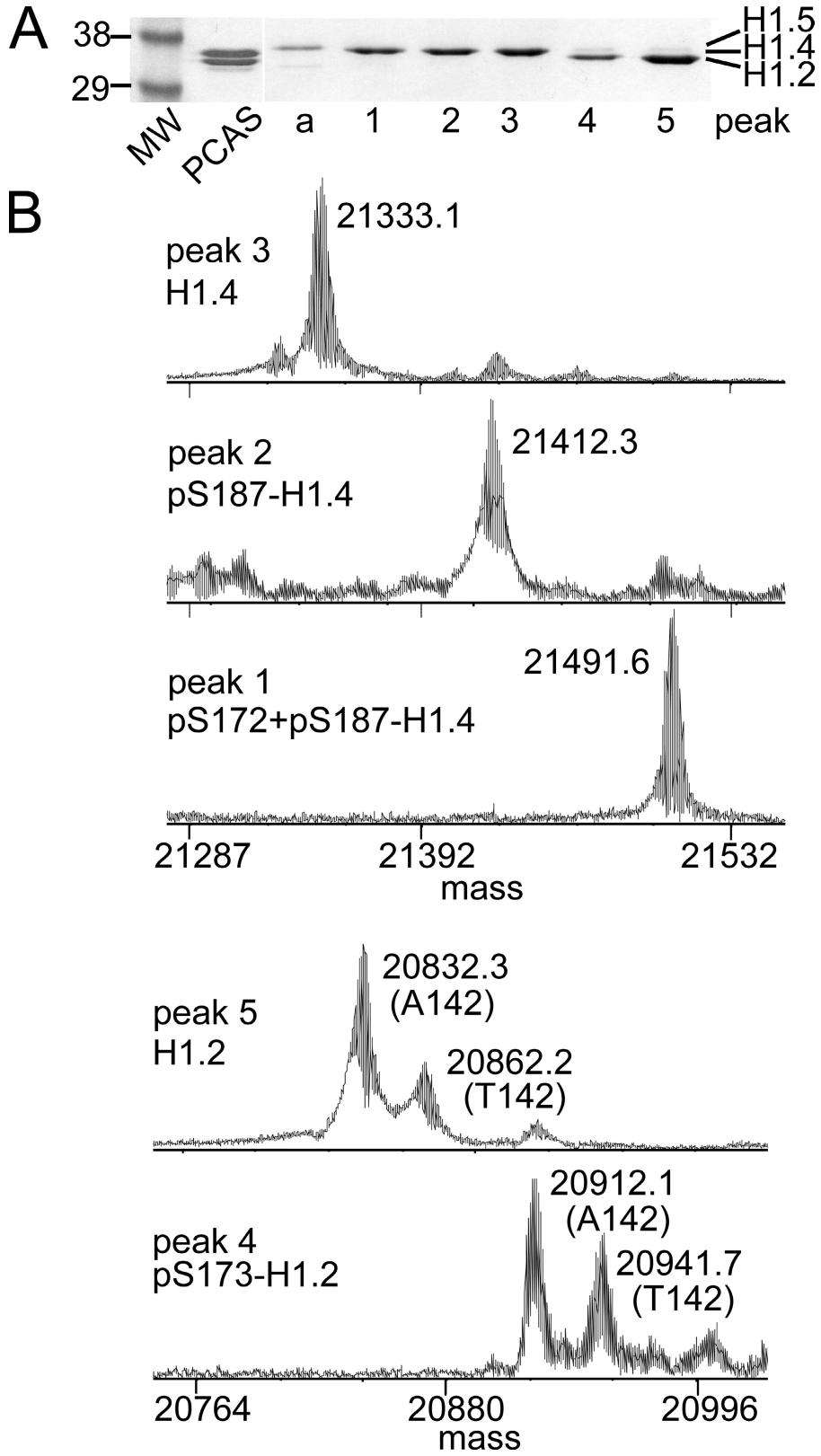

Figure S1. **Interphase phosphorylation of H1 variants is remarkably homogenous.** (A) SDS gel analysis of the HIC peaks for the mid–S phase sample shown in Fig. 1 B. The relative mobilities of H1.5 (pooled peaks a), H1.4 (peaks 1–3), and H1.2 (peaks 4 and 5) are shown on the right. Values are given in kilodaltons. PCAS, perchloric acid extracted crude H1 from asynchronous growing cells; MW, molecular weight. White line indicates that intervening

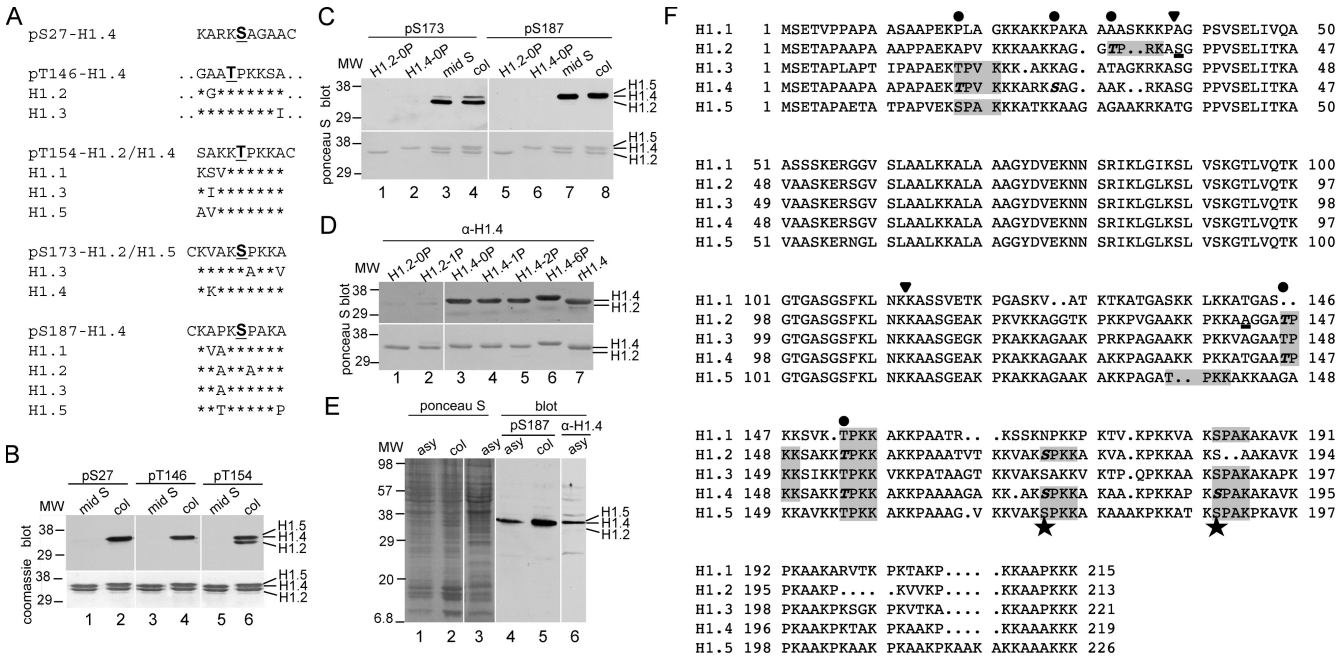

Figure S2. **Detection of individual mitotic and interphase phosphorylations by site-specific phosphopeptide antisera.** (A) Synthetic peptides representing the human pS27-H1.4, pT146-H1.4, and pT154-H1.2/H1.4 sites of mitotic phosphorylation and the pS173-H1.2/H1.5 and pS187-H1.4 sites of interphase phosphorylation were used to generate antisera in rabbits. Phosphorylated residues are shown in bold and underlined. Only the core portion of the peptide antigen used to generate antisera to pT146-H1.4 (Abcam) is shown. The corresponding Ser/Thr-containing motifs in other human H1 variants are shown below each antigen peptide. (B, top) Crude histones from mid–S phase (lanes 1, 3, and 5) and colchicine (col)-arrested HeLa S3 cells (lanes 2, 4, and 6) were analyzed by immunoblotting with antisera to pS27-H1.4, pT146-H1.4, or pT154-H1.2/H1.4. (bottom) Duplicate gels stained with Coomassie blue confirmed equivalent loading. In each case, bands were detected at the expected positions only in colchicine-arrested samples, suggesting that these three sites are phosphorylated exclusively in mitosis. (C, top) HPLC-purified nonphosphorylated H1.2 (H1.2-0p; lanes 1 and 5), H1.4-0p (lanes 2 and 6), crude histones from mid–S phase (lanes 3 and 7), and colchicine-arrested HeLa S3 cells (lanes 4 and 8) were analyzed by immunoblotting with antisera to pS173-H1.2/H1.5 or pS187-H1.4. (bottom) Ponceau S staining of the transfer membranes confirm equivalent loading. Both antisera detected bands at the expected positions in mid–S phase and colchicine-arrested samples (lanes 3, 4, 7, and 8), but nonphosphorylated H1.2/H1.4 was not detected (lanes 1, 2, 5, and 6). The weak signal apparent for H1.5 in lanes 3 and 4 is consistent with the low abundance of this variant in HeLa cells. (D, top) HPLC-purified H1.2-0p (lane 1), H1.2-1p (lane 2), H1.4-0p (lane 3), H1.4-1p (lane 4), H1.4-2p (lane 5), H1.4-6p (lane 6), and purified recombinant human H1.4 (rH1.4; lane 7) were analyzed by immunoblotting with antisera (α-H1.4) for total H1.4 that was raised against rH1.4. (bottom) Ponceau S staining of transfer membranes confirmed equivalent loading. The apparent affinity of the α-H1.4 antisera for native H1.4 with defined levels of phosphorylation (lanes 3–6) was similar to that for rH1.4 (lane 7), whereas binding to H1.2 was negligible (lanes 1 and 2). (E) Whole cell extracts of growing asynchronous (asy; lanes 1, 3, 4, and 6) and colchicine-treated cells (lanes 2 and 5) were analyzed by immunoblotting with antisera to pS187-H1.4 (lanes 4 and 5) or total H1.4 (lane 6). Ponceau S staining of transfer membranes confirmed equivalent loading (lanes 1–3). (F) The reference amino acid sequences of human H1.1 (NCBI Protein database accession no. NP_005316), H1.2 (NCBI Protein database accession no. NP_005310), H1.3 (NCBI Protein database accession no. NP_005311), H1.4 (NCBI Protein database accession no. NP_005312), and H1.5 (NCBI Protein database accession no. NP_005313) are shown aligned for maximum homology. Phosphorylation sites identified in this study are shown in bold italics. Circles above the sequences indicate sites presumed to be mitosis specific because they were only found to be phosphorylated in the tetraphosphorylated H1.2 (4p-H1.2) and hexaphosphorylated H1.4 (6p-H1.4) HIC peaks prepared from colchicine-treated cells (Fig. 1 B). Mitosis-specific phosphorylation was confirmed for several of these sites by immunostaining with site-specific antisera (see Materials and methods). Stars indicate H1.2-S173, H1.4-S172, and H1.4-S187 sites found to be phosphorylated during both interphase and mitosis. Arrowheads indicate the approximate boundaries of the globular domain of H1 (Cerf et al., 1994). Consensus sequences for phosphorylation by cyclin-dependent kinases are shown in gray. S36 and A142 of H1.2 are underlined to indicate the H1.2 gene nucleotide polymorphisms detected in HeLa S3 cells by genotyping. The polymorphism in the S36 codon is silent, but the polymorphism in the A142 codon generates the H1.2-T142 allelic variant that accounts for approximately one third to one fourth of total H1.2 in asynchronous cells (Fig. 1 A). (B–E) White lines indicate that intervening lanes have been spliced out. MW, molecular weight.

lanes have been spliced out. (B) The mass spectra of the HIC peaks for H1 from the mid–S phase sample shown in Fig. 1 B. Phosphorylation sites were identified by direct MS/MS analysis of electron capture dissociation fragment ions as described previously (Pesavento et al., 2008) and are listed in Table I. MS/MS analyses of the 20,862.2 D and 20,941.7 D forms of H1.2 observed for HIC peaks 5 and 4, respectively, localized a mass difference of ~30 D to H1.2 residues K127–K159. However, electron capture dissociation did not fragment this peptide further under the conditions used, preventing us from localizing the difference to a single residue. We then used gene-specific primers to amplify the H1.2 coding region from HeLa S3 cell genomic DNA, ligated the products into a bacterial vector, and sequenced plasmids recovered from multiple independent transformants. This approach detected two polymorphisms in the H1.2 gene that have not been described previously. The first is a silent T > C substitution at nucleotide 108 in the codon for Ser36 (TCT > TCC) that was observed in 30/30 clones analyzed. The second, a G > A substitution at nucleotide 424 in the codon for Ala142 (GCT > ACT), results in an Ala > Thr substitution. The predicted change in molecular mass (30.01 D) matches the 30-D difference observed for the K127–K159 fragment ion in the minor H1.2 forms described above. This polymorphism was observed in 8/30 of the H1.2 clones analyzed, a frequency that is similar to the relative abundances of the two components observed for unmodified H1.2 by MS for crude H1 (Fig. 1 A).

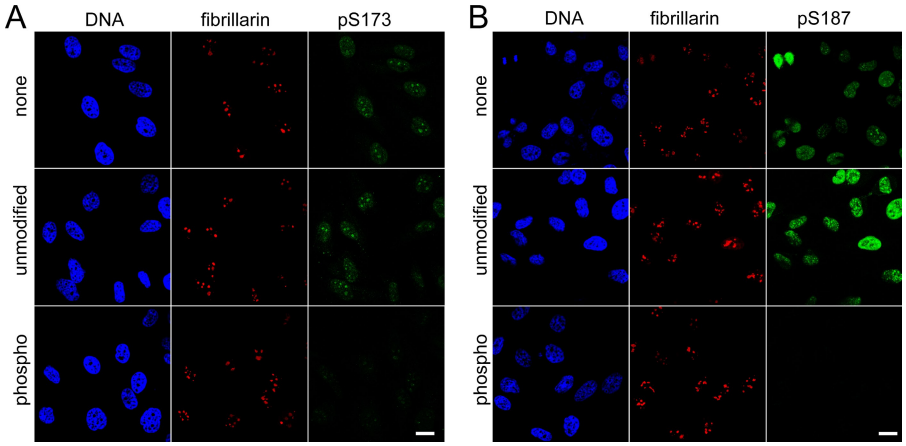

Figure S3. **Specificity of the pS173-H1.2 and pS187-H1.4 antisera in immunofluorescence microscopy.** (A) Crude antisera to pS173-H1.2/H1.5 was mock treated (no peptide) or preincubated with the pS173-H1.2/H1.5 antigen peptide (phospho) or the corresponding nonphosphorylated peptide (unmodified) before use in staining asynchronous growing HeLa cells. DNA and nucleoli were subsequently stained with TO-PRO-3 and antifibrillarin, respectively. (B) As in A except that crude antiserum to pS187-H1.4 and the corresponding peptides were used. Nuclear and nucleolar staining in both A and B were significantly reduced after preincubation with the respective phosphopeptide but was unaffected by preincubation with the nonphosphorylated peptide. Bars, 20 µm.

References

Cerf, C., G. Lippens, V. Ramakrishnan, S. Muyldermans, A. Segers, L. Wyns, S.J. Wodak, and K. Hallenga. 1994. Homo- and heteronuclear two-dimensional NMR studies of the globular domain of histone H1: full assignment, tertiary structure, and comparison with the globular domain of histone H5. *Biochemistry*. 33:11079–11086. doi:10.1021/bi00203a004

Pesavento, J.J., H. Yang, N.L. Kelleher, and C.A. Mizzen. 2008. Certain and progressive methylation of histone H4 at lysine 20 during the cell cycle. *Mol. Cell. Biol.* 28:468–486. doi:10.1128/MCB.01517-07